Methane emissions offset net carbon dioxide uptake from an alpine peatland on the Eastern Qinghai-Tibetan Plateau

Haijun Peng[a,d,e], Jinshu Chi[b,*], Hu Yao[a,c,d], Qian Guo[a,c,d], Bing Hong[a,d,e,*], Hanwei Ding[a,c,d], Yongxuan Zhu[a], Jie Wang[a,c,d], Yetang Hong[a]

[a] State Key Laboratory of Environmental Geochemistry, Institute of Geochemistry, Chinese Academy of Sciences, Guiyang 550081, China

[b] Department of Forest Ecology and Management, Swedish University of Agricultural Sciences, Umeå, 90183, Sweden

[c] University of Chinese Academy of Sciences, Beijing 100049, China

[d] Bayinbuluk alpine wetland carbon flux research station, Chinese Flux Observation and Research Network

[e] CAS Center for Excellence in Quaternary Science and Global Change, Xi'an, 710061, China

[*] Correspondence to J. Chi (jinshu.chi@slu.se) and B. Hong (hongbing@mail.gyig.ac.cn)

Key Points:

- CH_4 emissions offset the net CO_2 uptake from an alpine peatland on eastern QTP
- The alpine peatland showed a net radiative warming effect
- Soil temperature and global radiation were dominant abiotic controls of net CO_2-eq flux variations

Abstract

Peatlands store large amounts of carbon (C) and actively exchange greenhouse gases (GHGs) with the atmosphere, thus playing an important role in global C cycle and climate. Large uncertainty exists in estimating C and GHG budgets of the alpine peatlands on Qinghai-Tibetan Plateau (QTP), as direct measurements of carbon dioxide (CO_2) and methane (CH_4) fluxes are still scarce in this region. In this study, we provided ~2.5-year continuous CO_2 and CH_4 fluxes measured using the eddy covariance technique in a typical alpine peatland on the eastern QTP to estimate the net C and CO_2-eq fluxes and investigate their environmental controls. Our results showed that the mean annual CO_2 and CH_4 fluxes were -106 g C-CO_2 m^{-2} yr^{-1} and 35 g C-CH_4 m^{-2} yr^{-1}, respectively. While considering the traditional and sustained global warming potentials of CH_4 over the 100-year time scale, the peatland acted as a net source of CO_2-eq (918 and 1712 g CO_2-eq m^{-2} yr^{-1}, respectively). The net CO_2-eq emissions during the non-growing seasons contributed to over 40% of the annual CO_2-eq budgets. We further found that the net CO_2-eq flux was primarily influenced by soil temperature and global radiation variations. This study was the first assessment to quantify the net CO_2-eq flux of the alpine peatland in the QTP region using long-term eddy covariance measurements. Our study highlights that CH_4 emissions from peatlands can largely offset the net cooling effect of CO_2 uptake and future climate changes such as global warming might further enhance their potential warming effect.

Keywords: Peatlands, radiative forcing, greenhouse gas fluxes, carbon budgets, eddy covariance, Qinghai-Tibetan Plateau

1. Introduction

Carbon dioxide (CO_2) and methane (CH_4) are the two most important long-lived greenhouse gases (LLGHGs) and together contribute to over 80% of the radiative forcing caused by LLGHGs [*WMO*, 2018]. Peatlands cover only about 3% of the Earth's land surface area but store over 500 Pg (10^{15} g) of carbon (C), accounting for one-third of the global soil C pool and about 70% of the atmospheric C pool [*Gorham*, 1991; *Loisel et al.*, 2017; *Turunen et al.*, 2002; *Yu et al.*, 2010]. It has been widely acknowledged that peatlands have played an important role in regulating the global C and GHG cycles and climate change [*Friedlingstein et al.*, 2019; *Frolking et al.*, 2011; *Hopple et al.*, 2020]. Peatland ecosystems have the potential to mitigate climate change by sequestering CO_2 from the atmosphere into biomass and soils [*Baldocchi and Penuelas*, 2019; *Nugent et al.*, 2019; *Stocker et al.*, 2017]; meanwhile, peatlands emit large amounts of CH_4 to the atmosphere during the peatland forming and growing processes [*Dommain et al.*, 2018; *Kirschke et al.*, 2013], thus resulting in contrasting effects on radiative forcing. Both pathways are sensitive to climate change and anthropogenic activities [*Chen et al.*, 2013; *Frolking et al.*, 2011]; for examples, drought caused by both peatland drainage and low precipitation [*Fenner and Freeman*, 2011; *Swindles et al.*, 2019], peatland wildfires and burning [*Turetsky et al.*, 2015], and conversion for agricultural uses [*Carlson et al.*, 2013; *Dommain et al.*, 2018] can shift the peatlands from net GHG sinks to sources. However, it should be noted that the historical, current, and future contributions of peatlands to the global C budget and radiative forcing are still uncertain due to limited knowledge of the synergistic feedbacks of CO_2 and CH_4 to climatic perturbation and anthropogenic activities [*Luan et al.*, 2018; *Petrescu et al.*, 2015; *Stocker et al.*, 2017].

The uncertainty in CO_2 and CH_4 stoichiometry of peatlands could be attributed to a variety of sources, such as the lack of reliable global peatland area estimates [*Chaudhary et al.*, 2017; *Xu et al.*, 2018; *Yu et al.*, 2010], difficulties in quantifying terrestrial anaerobic or oxidative sources and sinks [*Bridgham et al.*, 2013; *Loisel et al.*, 2017; *Poulter et al.*, 2017], and the scarcity of both CO_2 and CH_4 flux measurements, especially from low-latitude and high-altitude peatlands [*Bridgham et al.*, 2013; *Kirschke et al.*, 2013; *Schaefer et al.*, 2016; *Yu et al.*, 2010]. To date, most of the peatland C fluxes have been measured in the northern high-latitude (45-70°N) [*Loisel et al.*, 2017; *Turetsky et al.*, 2014]. Recent studies show that wetland ecosystems in the subtropical and tropical regions have acted as C sinks, but their CH_4 emissions can offset net CO_2 uptake under warm scenarios, thus contributing to a positive radiative forcing [*Dalmagro et al.*, 2019; *Dommain et al.*, 2018; *Liu et al.*, 2020]. Considering peatlands in the low-latitude regions have a sizeable amount of C stocks and higher CH_4 emissions and C sequestration rates compared to the northern peatlands [*Loisel et al.*, 2017; *Nilsson et al.*, 2008; *Yu et al.*, 2010], the lack of C flux measurements from these areas could lead to large uncertainty in the global peatland C and GHG budget estimations [*X Liu et al.*, 2019; *Schaefer et al.*, 2016; *Turetsky et al.*, 2015]. Therefore, more monitoring is needed to reveal the dynamics in peatland-atmosphere C exchanges and dynamics.

The Ruoergai peatland in the eastern margin of the Qinghai-Tibetan Plateau (QTP) is the largest consecutive alpine peatland in the world, covering a total area of 4600 km^2 at an average elevation of 3400 meters above sea level [*Chen et al.*, 2014; *Xiang et al.*, 2009; *Yao et al.*, 2011]. The climate of the eastern QTP is influenced by the Asian monsoons and characterized by short, warm, and wet summer with high solar irradiation and long, cold, and dry winter, which promotes the growth of herbaceous plants and preserving of peat or organic material rich soils

[*Hong et al.*, 2005; *Peng et al.*, 2015]. The mean annual temperature in the QTP region has been rapidly increasing at a rate of 0.27 ℃ per decade during 1961-2005, whereas global mean surface temperature has risen only by 0.85 ℃ since 1880 [*Tang et al.*, 2018; *You et al.*, 2016]. Due to the rapid warming, glacier melting and retreats have provided more water for peatland formation despite precipitation in the QTP region has not changed dramatically [*Yao et al.*, 2012]. As the biogeochemical processes regulating the CO_2 and CH_4 flux magnitudes are temperature-dependent and sensitive to water availability [*Hopple et al.*, 2020; *Peichl et al.*, 2014; *Yuan et al.*, 2011; *Yvon-Durocher et al.*, 2014], both fluxes have significantly been altered due to climate change in the QTP region [*Chen et al.*, 2013; *Yang et al.*, 2014].

Temporal patterns of CO_2 or CH_4 fluxes and their dominant environmental controls have been recently but separately explored over the Ruoergai peatland [*Chen et al.*, 2021; *X Liu et al.*, 2019; *Peng et al.*, 2019]. However, studies into ecosystem-level net CO_2 equivalent flux (net CO_2-eq flux, i.e., summing up CO_2 and CH_4 fluxes weighted by different global warming potential metrics of CH_4) and its overall environmental controls are still rare in this region. In this study, we compiled ~2.5-year (32 months) continuous eddy covariance (EC) measurements of CO_2 and CH_4 fluxes at a typical alpine peatland on the eastern QTP to (a) characterize the temporal variations of net ecosystem exchanges of CO_2, CH_4, and their CO_2 equivalents between the alpine peatland and the atmosphere; (b) investigate the biophysical drivers of the net CO_2-eq fluxes at different temporal scales; and (c) assess the overall net radiative forcing arising from sustained CH_4 emissions and concurrent net CO_2 uptake from the alpine peatland on the eastern QTP. To our knowledge, this study was the first to present a multi-year continuous dataset of ecosystem-scale CO_2 and CH_4 fluxes over alpine peatlands on QTP, providing key information for understanding the role of alpine peatlands in the global C balance and net radiative forcing.

2. Methods

2.1. Site description

The study site is at the Hongyuan Peatland Carbon Flux Monitoring and Research Station (32°46' N, 102°30' E, 3510 m.a.s.l.) operated by the Institute of Geochemistry, Chinese Academy of Sciences. The site is located in a valley on the eastern side of the Bai River in Hongyuan County, Sichuan Province, China (Figure 1). The Hongyuan peatland has an area of 1.1 km^2 and the deepest peat deposition is around 6.5 m. It is a part of the Ruoergai wetland, which covers 15% of the Ruoergai Basin area on the eastern QTP [*Peng et al.*, 2019; *Yao et al.*, 2011] and stores approximately 0.48 Pg C, some of which have been formed since 15,000 years ago [*Chen et al.*, 2014]. The long-term (1981-2010) meteorological data from the National Benchmark Climate Station in Hongyuan (http://data.cma.cn/) showed that the mean annual temperature and precipitation are 1.8 °C and 746 mm, respectively. The highest monthly mean air temperature is typically observed in July (11.2 °C on average), whereas the lowest is in January with a 30-year mean of -9.4 °C. More than 75% of annual precipitation usually occurs during the growing season from May to September each year. The dominant plant species in Hongyuan peatland are *Carex mulieensis* and *Kobresia tibetica*, and other abundant plant species include *Caltha palustris*, *Gentiana formosa*, and *Trollius farreri*.

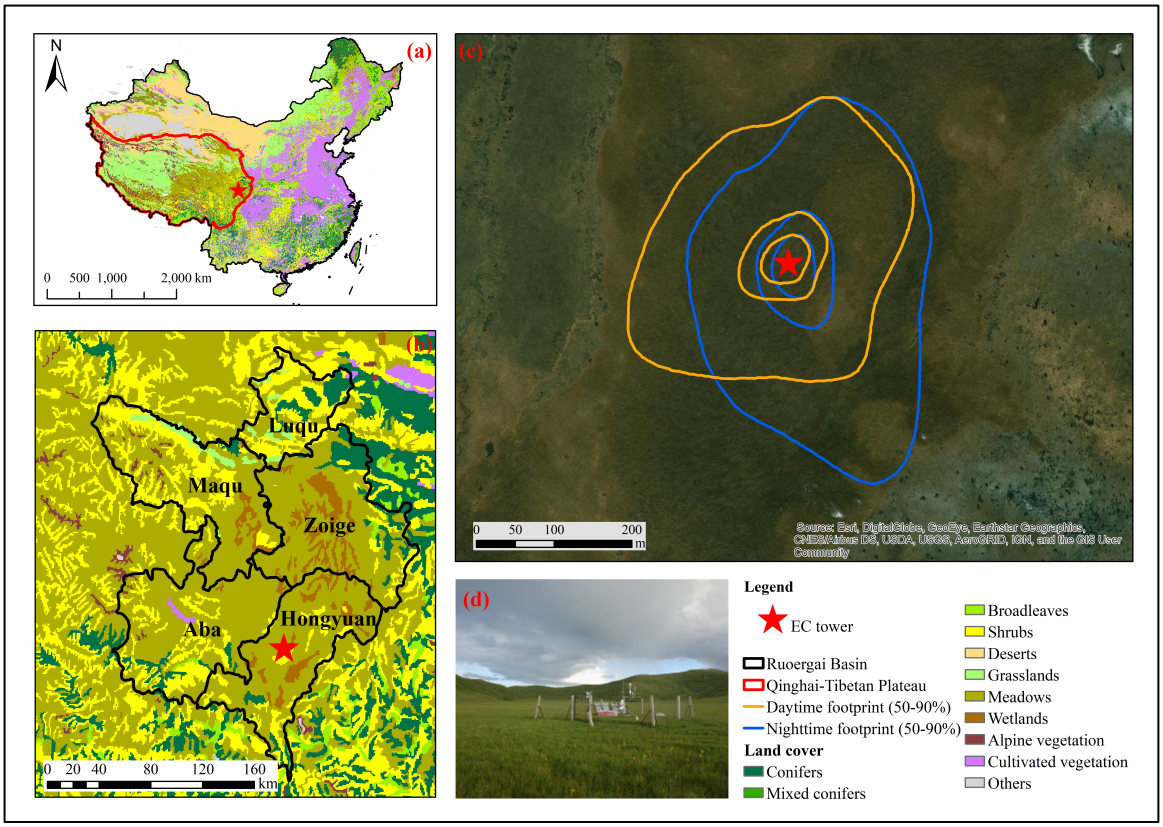

Figure 1: Location of the eddy covariance flux tower at Hongyuan peatland on the eastern Qinghai-Tibetan Plateau and its flux measurement footprint during daytime (orange lines) and nighttime (blue lines). The land cover data in panels (a) and (b) were retrieved from the Data Center for Resources and Environmental Sciences of the Chinese Academy of Sciences (http://www.csdb.cn). The footprint contour lines in panel (c) are shown in increments of 20% from 50% (inner circle) to 90% (outer circle).

2.2. Eddy covariance and ancillary measurements

The EC tower was installed in the center of Hongyuan peatland, where the terrain is flat and the average peat depth is 3.3 m. The flat area has a diameter of > 300 m, which provides a homogeneous upwind fetch for the EC flux measurements (Figure 1). The EC sensors were mounted at 2.5 m above the ground, consisting of a 3-D ultrasonic anemometer (WindMaster Pro, Gill Instruments Limited, UK) for measuring wind components, an open-path infrared gas analyzer (LI-7500A, LI-COR Biosciences, USA) for measuring carbon dioxide and water vapor densities, and an open-path gas analyzer (LI-7700, LI-COR Biosciences, USA) for measuring CH_4 concentrations. The LI-7500A was tilted 10° in the main wind direction to avoid water

accumulation on the lens. The raw EC data were recorded at 10 Hz using the LI-7550 data logger (LI-7700, LI-COR Biosciences, USA). Other ancillary environmental measurements, including global radiation (R_g), air temperature (T_{air}) and relative humidity (RH), precipitation (PPT), soil temperature (T_{soil}) at three depths (10, 25, and 40 cm below the ground), and soil water content (SWC) at a depth of 10 cm, were recorded by a HOBO U30 weather station installed near the EC tower (Figure 1). Vapor pressure deficit (VPD) was calculated using the T_{air} and RH measurements. The EC tower was powered by solar panels during daytime and lead-acid batteries during nighttime or when solar radiation was low. A more detailed description of instrumentation is presented in *Peng et al.* [2019].

2.3. Flux data processing and radiative forcing calculation

The 10 Hz EC raw data were processed using the express mode in EddyPro® software (Version 5.1.1, LI-COR Biosciences, USA) to obtain the half-hourly averaged fluxes of CO_2 and CH_4. A detailed description of raw flux calculation was presented in *Peng et al.* [2019] and thus was not repeated in this study. In brief, double rotation [*Wilczak et al.*, 2001], block average [*Gash and Culf*, 1996], and covariance maximization [*Fan et al.*, 1990] were applied in the EddyPro settings. Flux data were corrected for spectral attenuations [*Moncrieff et al.*, 2004; *Moncrieff et al.*, 1997] and density fluctuations [*Webb et al.*, 1980]. The 30-min CO_2 and CH_4 flux data were filtered according to the EddyPro "0-1-2" quality check flagging policy [*Mauder and Foken*, 2004] that data with a flag of "2" were discarded. As spikes still occurred in the time series data, half-hourly CO_2 and CH_4 fluxes were further removed if they were outside the range of mean ± 3×standard deviation over a moving window of 10 days. Moreover, the half-hourly CO_2 and CH_4 fluxes measured during the calm and stable atmospheric conditions, indicated by low friction

velocity (u_*) were discarded via the REddyProc online tool [*Wutzler et al.*, 2018] following the procedures described in *Papale et al.* [2006]. The u_* thresholds ranged from 0.082 to 0.147 m s^{-1} at our site.

Gaps in CO_2 flux were filled using the marginal distribution sampling (MDS) method [*Reichstein et al.*, 2005] implemented in the REddyProc online tool. The MDS look-up table variables include global radiation, air temperature, and vapor pressure deficit. As CH_4 emissions are widely found to be controlled by soil temperature and water table level [e.g., *Chen et al.*, 2021; *Rinne et al.*, 2018; *Ueyama et al.*, 2020], the CH_4 flux data were gap-filled by the regression fitting approach using soil temperature and soil water content as environmental drivers. More details are provided in our previous study [*Peng et al.*, 2019]. The micrometeorological sign convention was used in this study that positive and negative fluxes indicated emission from and uptake by the peatland ecosystem, respectively.

The net radiative forcing of Hongyuan peatland was computed as the sum of the vertical CO_2 and CH_4 fluxes in CO_2 equivalents (defined as net CO_2-eq flux) weighted by global warming potential (GWP) of CH_4. We applied both the traditional and sustained GWP (SGWP) metrics, the latter of which has been recently used to determine the net radiative forcing of several ecosystems by considering their persistent GHG emissions rather than the isolated pulse emissions [e.g., *Hemes et al.*, 2018; *Hemes et al.*, 2019; *Liu et al.*, 2020]. In this study, we chose the CH_4 GWP of 28 CO_2-eq (GWP-28) without the inclusion of climate-carbon feedbacks [*Myhre et al.*, 2013] and the SGWP of 45 CO_2-eq (SGWP-45) [*Neubauer and Megonigal*, 2015] over the 100-year time horizon. A positive net CO_2-eq value indicates an overall climatic warming effect and *vice versa*.

191 2.4. Statistical and footprint analyses

192 Principle component analysis (PCA) was performed on the time-series data at the temporal
193 resolutions of 30-min (non-gapfilled), daily, and monthly to investigate the correlation structures
194 of the CO_2, CH_4, and net CO_2-eq fluxes with the environmental variables. Flux measurement
195 footprint was estimated using the two-dimensional footprint parametrization [*Kljun et al.*, 2015].
196 Roughness length (z_0) and zero-plane displacement height (d) were estimated as 1/10 and 2/3 of
197 the canopy height (0.1 m), respectively. Besides, other footprint model input includes wind
198 direction, standard deviation of lateral wind component fluctuations, friction velocity, Monin-
199 Obukhov length, and atmospheric boundary layer height, i.e., 800 m and 200 m for daytime and
200 nighttime condition, respectively, for the eastern QTP region [*Slättberg and Chen*, 2020].

201

202 2.5. Evaluation periods

203 During the study period from December 2013 to July 2016, the annual period is defined as the
204 calendar year, which is further divided into four seasons, i.e., soil thawing (ST), growing season
205 (GS), soil freezing (SF), and winter (W) based on the approaches described in *Aurela et al.*
206 [2002] and *Lund et al.* [2010]. The starting and ending dates for each season during the study
207 period were listed in the supplemental materials (Table S1).

208

209 **3. Results**

210 3.1. Environmental conditions

211 The environmental conditions showed distinct characteristics between the two full annual
212 periods (Figure 2). As shown in Figure 2a, T_{air} did not differ much between the two years ($p >$
213 0.05), but the mean R_g during 2015 was significantly larger than in 2014 ($p < 0.05$), especially

during the growing season. Compared to 2014, the year of 2015 was identified as a relatively drier year, with 182 mm less PPT occurring during the growing season. However, the cumulative PPT during the first half of the growing season (May-July) was similar in 2014 and 2015 (316 vs. 334 mm), and thus the largely reduced PPT mainly occurred from August 2015 (Figure 2b). During the first half of the growing season, T_{soil} at the depth of 10 cm decreased by 1.0 °C from 2014 to 2015, forming a cooler and wetter soil condition over that period due to a slight increase in PPT. In contrast to the growing season, T_{soil} at 10 cm deep was 1.8 times higher across the entire non-growing season in 2015 compared to 2014. As expected, SWC mainly varied with PPT throughout the study period (Figure 2c).

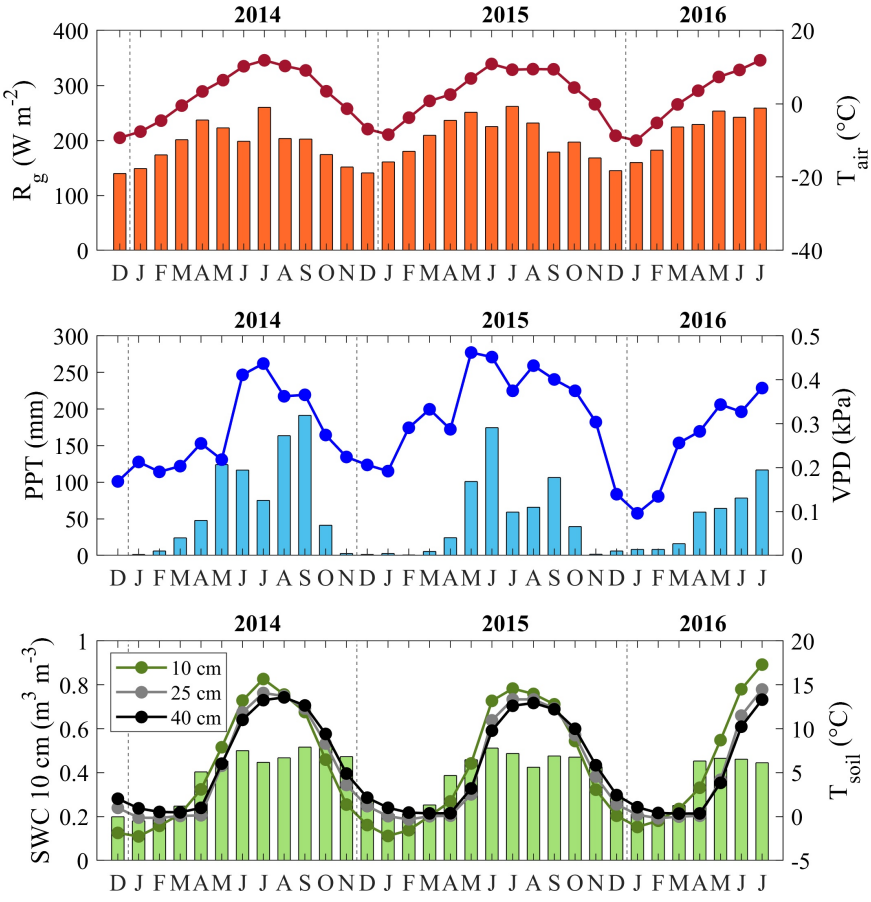

Figure 2: Monthly means (or sums) of environmental variables during the study period from December 2013 to July 2016 at Hongyuan peatland. (a) Monthly mean global radiation (R_g, red bars) and air temperature (T_{air}, red dots); (b) monthly precipitation sums (PPT, cyan bars) and monthly mean vapor pressure deficit (VPD, blue dots); and (c) monthly mean soil water content at a depth of 10 cm (SWC,

green bars) and soil temperature (T_{soil}) at the depths of 10 cm (green dots), 25 cm (grey dots), and 40 cm (black dots).

3.2. Temporal patterns of CO_2 and CH_4 fluxes

The measurements of net CO_2 and CH_4 exchanges between Hongyuan peatland and the atmosphere extended across two full annual periods and ~2.5 growing seasons from December 2013 to July 2016 (Figure 3). The peatland was a net CO_2 sink from May or June to September each year but a net source of CH_4 throughout the entire study period. Combining both CO_2 and CH_4 fluxes into CO_2 equivalents using the GWP-28 metric, the peatland acted as a net source of CO_2-eq fluxes for 10 and 11 months during 2014 and 2015, respectively. The peak net CO_2-eq uptake concurred with the largest CO_2 uptake in July each year, around which the highest monthly CH_4 fluxes were also observed, i.e., in August 2014, July 2015, and July 2016. The peak net CO_2-eq emission was observed at the end of the growing season each year, i.e., September 2014 and October 2015. While applying the SGWP-45 metric, the monthly net CO_2-eq fluxes were all positive throughout the entire measurement period, illustrating that the peatland was a net source of net CO_2-eq consistently in each month (Figure S1).

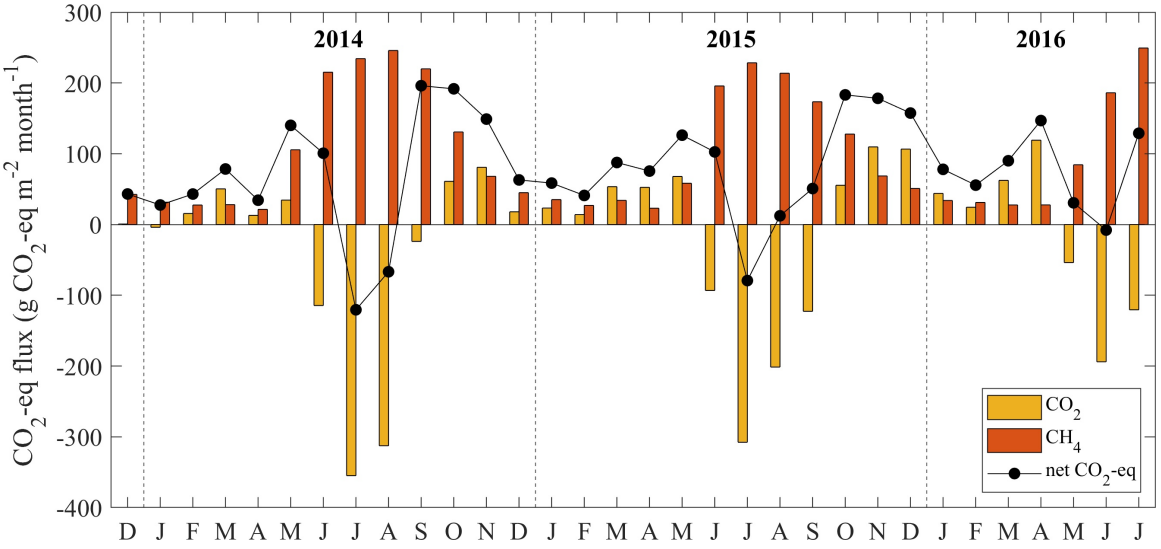

Figure 3: Monthly sums of CO_2, CH_4, and net CO_2-eq (GWP-28) fluxes over the study period from December 2013 to July 2016 at Hongyuan peatland. All flux components are in g CO_2-eq m^{-2} $month^{-1}$ using CH_4 traditional global warming potential of 28 (GWP-28).

3.3. Seasonal, annual, and between-year variability of CO_2-eq fluxes

The net CO_2-eq flux (GWP-28) during the soil freezing period accounted for >40% of the annual net CO_2-eq value (GWP-28), exceeding the contribution from the growing season by 10-20% each year (Table 1). Moreover, the net CO_2-eq (GWP-28) emission during the wintertime was 17% and 21% of the annual CO_2-eq sums during 2014 and 2015, respectively. In both years, the minimum contribution originated from the soil thawing period, which was also the shortest season (Table S1), were only 10% and 17% for 2014 and 2015, respectively. In contrast, the SGWP-45 metric showed the most significant net CO_2-eq emissions occurring during the growing seasons, 54% and 44% during 2014 and 2015, respectively (Table 1).

Table 1: Seasonal and annual CO_2 and CH_4 fluxes, and their CO_2 equivalents at Hongyuan peatland

		CO_2 flux		**CH_4 flux**			**Net C or CO_2-eq flux**		
	Year	g C m^{-2}	g CO_2 m^{-2}	g C m^{-2}	g CO_2-eq m^{-2} (GWP-28)	g CO_2-eq m^{-2} (SGWP-45)	g C m^{-2}	g CO_2-eq m^{-2} (GWP-28)	g CO_2-eq m^{-2} (SGWP-45)
A*	2014	-146	-535	37	1381	2220	-109	846	1685
	2015	-66	-242	33	1232	1980	-33	990	1738
ST	2014	14	51	0.8	30	48	15	81	99
	2015	33	121	1.3	49	78	34	170	199
GS	2014	-209	-766	28	1045	1680	-181	279	914
	2015	-186	-682	24	896	1440	-162	214	758
SF	2014	39	143	5.3	198	318	44	341	461
	2015	60	220	4.9	183	294	65	403	514
W	2014	10	37	2.9	108	174	13	145	211
	2015	27	99	2.8	105	168	30	204	267

** Abbreviations: annual (A), soil thawing (ST), growing season (GS), soil freezing (SF), and winter (W).*

For each annual period, Hongyuan peatland acted as a sink for atmospheric CO_2 but a source of CH_4 to the atmosphere (Table 1). While considering the GWP-28 of CH_4, the annual CO_2-eq flux was 846 and 990 g CO_2-eq m^{-2} yr^{-1} during 2014 and 2015, respectively, which was

almost doubled when applying the SGWP-45 metric (Table 1). The increased annual net CO_2-eq emission during 2015 corresponded with the largely reduced CO_2 uptake and slightly lower CH_4 emission, compared to the year of 2014.

3.4. Controlling factors of net CO_2-eq flux

During the study period, the net CO_2-eq flux was dominantly varied with the CO_2 flux component at half-hourly ($r = 0.98$, $p < 0.001$), daily ($r = 0.86$, $p < 0.001$), and monthly time scales ($r = 0.77$, $p < 0.001$), whereas little correlation existed between net CO_2-eq and CH_4 flux at all three temporal scales (Figure 4). The negative correlation between CO_2 and CH_4 fluxes, representing a positive correlation between CO_2 uptake and CH_4 emissions, increased from half-hourly to monthly scales (Figure 4d-f).

Among the six investigated environmental variables, R_g and T_{soil} were the strongest controlling factor of the half-hourly CO_2 and CH_4 fluxes, respectively (Figure 4a&4d). At the coarser temporal resolutions, i.e., daily and monthly timescales, T_{soil} became the most influencing abiotic control of both CO_2 and CH_4 fluxes (Figure 4b, c, e, f). Overall, R_g and T_{soil} were the dominant environmental factors influencing net CO_2-eq fluxes (GWP-28) at half-hourly and daily intervals; however, no significant environmental control was found for the monthly net CO_2-eq flux (Figure 4f). Following the SWGP-45 metric, the correlation structures did not vary much from the GWP-28 metric, except that SWC was significantly correlated with the monthly net CO_2-eq fluxes (Figure S2).

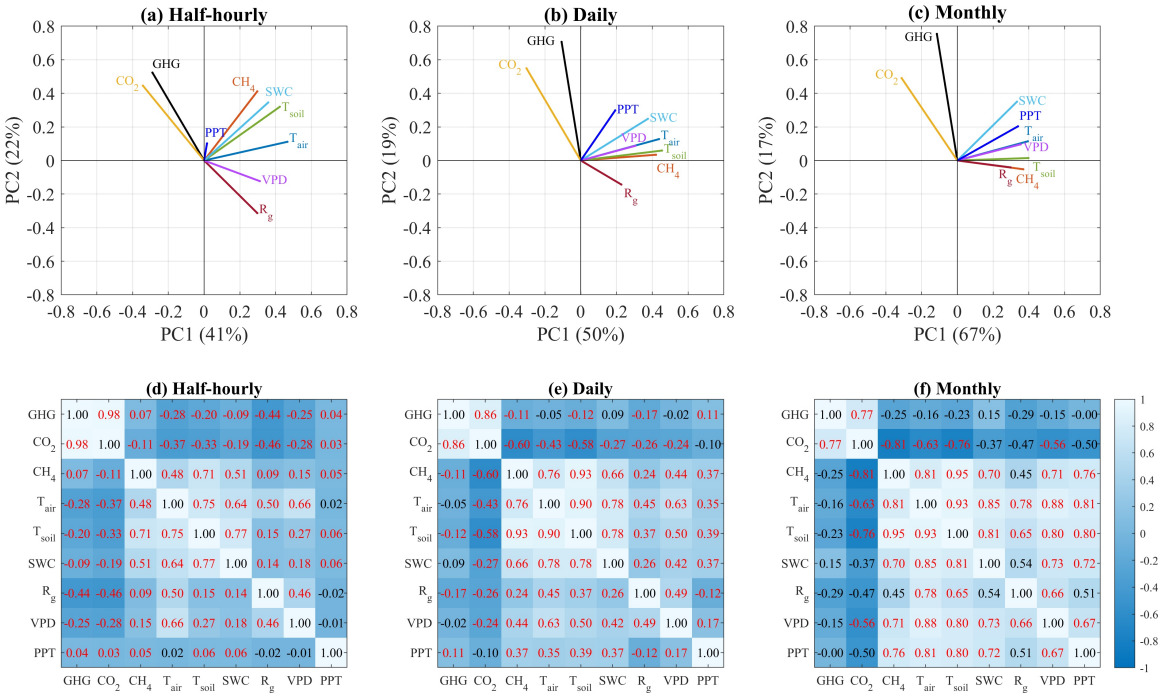

Figure 4: PCA loading plots (a-c) of the correlation structures of GHG (net CO_2-eq, GWP-28), CO_2, and CH_4 (CO_2-eq, GWP-28) fluxes, and measured environmental variables and their correlation matrix (d-e) at half-hourly, daily, and monthly temporal scales. Environmental variables include global radiation (R_g), air temperature (T_{air}), precipitation (PPT), vapor pressure deficit (VPD), and soil temperature (T_{soil}) and soil water content (SWC) both at the depth of 10 cm measured during the study period from December 2013 to July 2016 at Hongyuan peatland. Values in the correlation matrix are the correlation coefficients and significant correlations ($p < 0.001$) are labeled using the red fonts.

During the growing season, bin-averaged responses of net CO_2-eq fluxes to different R_g classes illustrated that the net CO_2-eq uptake (negative CO_2-eq flux) was significantly enhanced by the increasing R_g before reaching light saturation where R_g was around 500 W m^{-2} (Figure 5a). Meanwhile, T_{air} (5-15 °C) and PPT positively affected the net CO_2-eq uptake and emission rates, respectively (Figure 5b and 5c). The relationship between net CO_2-eq flux and VPD showed that the net CO_2-eq uptake quickly increased with VPD up to a threshold of ~0.66 kPa, beyond which the net CO_2-eq uptake started to decrease (Figure 5d). Additionally, the net CO_2-eq flux during the growing season showed similar responses to T_{soil} (> 5 °C) and SWC (> 0.44 m^3 m^{-3}) as to T_{air} and PPT, respectively (Figure 5e and 5f). During the non-growing seasons, net

CO_2-eq generally increased with T_{soil} and the lower SWC range (e.g., 0.16-0.28 m^3 m^{-3}) (Figure 5e and 5f).

As the CO_2 flux component was dominantly driving the variations in net CO_2-eq fluxes, its sensitivity to the environmental parameters was similar to the responses of net CO_2-eq flux (Figure S3). Whereas for CH_4 flux, we observed that CH_4 emissions during the growing season were linearly increasing with T_{soil} and exponentially increasing with T_{air}, which were also inhibited at the high VPD range (> 1.7 kPa) (Figure S4). Moreover, CH_4 emission sensitivities to R_g, T_{soil}, and SWC were noted only during the soil freezing period. The environmental responses of net CO_2-eq fluxes for the SGWP-45 metric did not differ much from the GWP-28 metric (Figure S5).

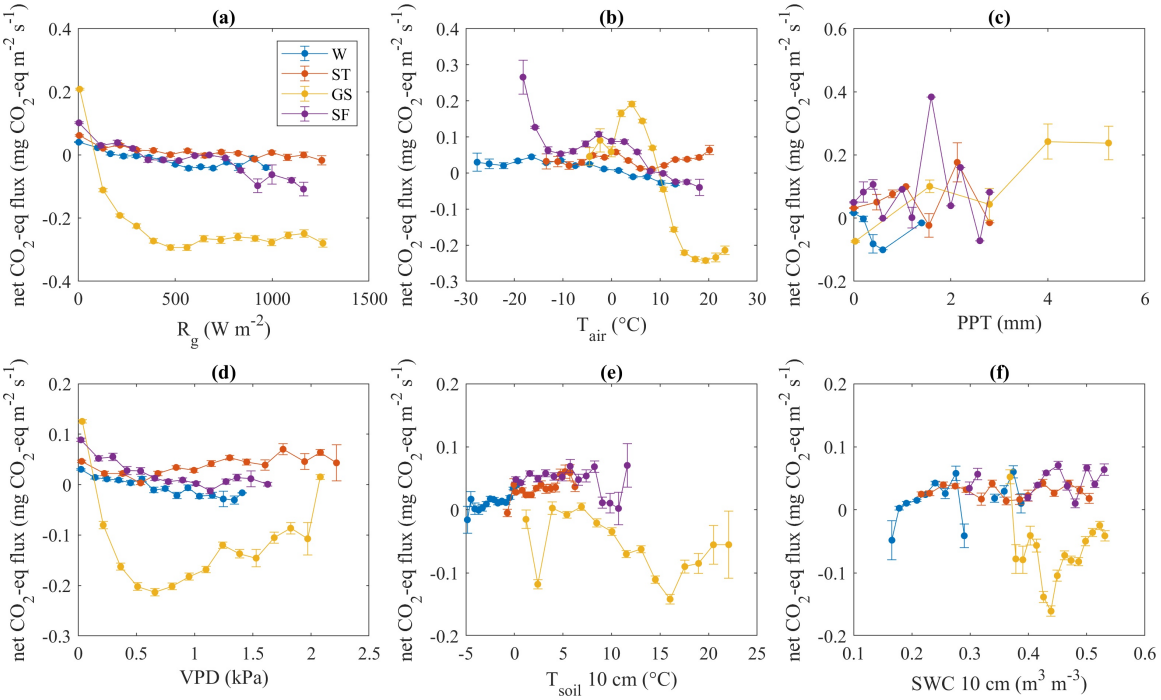

Figure 5: Bin-averaged half-hourly net CO_2-eq flux against environmental variables during the periods of winter (W), soil thawing (ST), growing season (GS), and soil freezing (SF) at Hongyuan peatland. The error bars show the standard errors of the bin averages.

4. Discussion

4.1. CH_4 emissions offset the net cooling effect of CO_2 uptake

On an annual basis, our CO_2 and CH_4 flux measurements demonstrated that Hongyuan peatland was a net sink for atmospheric CO_2, a source of atmospheric CH_4, and an overall net C sink. The mean annual net C sink strength (71 g C m^{-2} yr^{-1}) during the study period was within the range of C accumulation rates (35-171 g C m^{-2} yr^{-1}) during the recent decades for the alpine peatlands in the Ruoergai Basin [e.g., *Hao et al.*, 2011; *X Liu et al.*, 2019; *Wang et al.*, 2015], which further confirms that the recent C accumulation rates of peatlands in this region are almost four times larger than their Holocene averaged values [*Wang et al.*, 2015; *Zhao et al.*, 2014]. Within the C balance, C loss via CH_4 emissions was relatively lower compared to the magnitude of net CO_2 uptake.

While considering the GWP and SGWP of CH_4 over the 100-year time scale, CH_4 emissions have exceeded the net cooling effect of CO_2 uptake by 2.5-4 times each year, resulting in the net positive radiative forcing and a potential warming effect of Hongyuan peatland. Moreover, considering the net positive radiative forcing is ~4 times stronger regarding the GWP and SGWP of CH_4 over the 20-year time horizon (84 and 96, respectively), the GHG emissions from Hongyuan peatland would have a more substantial warming effect over a shorter time scale. The consistently positive annual net CO_2-eq fluxes estimated using two different GWP metrics over both short- and long-time scales revealed that CH_4 emissions from the alpine peatlands are a crucial land-atmosphere C exchange component in the net CO_2-eq flux and greenhouse gas budgets.

A large portion (~60% and 40% for GWP-28 and SGWP-45) of the annual net CO_2-eq flux was observed during the soil freezing and winter periods when the environmental conditions were unfavorable for plant growth. During these cold periods, soil respiration was expected to be

342 the dominant process that released CO_2 into the atmosphere [*X Liu et al.*, 2019] and meanwhile
343 the peatland was still emitting CH_4 via anaerobic decomposition of soil organic matters [*Peng et*
344 *al.*, 2019]. Moreover, winter was not dormant in terms of CO_2 and CH_4 production, even though
345 T_{soil} at 10 cm depth and T_{air} dropped below zero for 98% and 76% of the wintertime of 2014 and
346 2015, respectively. During the wintertime, CO_2 and CH_4 emissions from peatlands can still occur
347 through the frozen or snow-covered soils via diffusion and transportation through the chimney
348 effect led by dead plant tissues and ice cracks and also through the burst emissions caused by
349 rapid soil thawing and freezing [*Alm et al.*, 1999; *Mastepanov et al.*, 2008; *Song et al.*, 2020].
350 The important CO_2-eq emission during the non-growing season was in accordance with previous
351 studies, which have recently highlighted that the overall C and GHG budgets may be
352 underestimated without an accurate assessment for the non-growing season [*Aurela et al.*, 2002;
353 *Commane et al.*, 2017; *Natali et al.*, 2019; *Song et al.*, 2015].
354
355 4.2. Abiotic controls of net CO_2-eq flux
356 Compared to 2014, the largely enhanced annual CO_2-eq source strength during 2015 was
357 attributed to the elevated CO_2-eq emissions during the non-growing season and slightly reduced
358 net CO_2 uptake during the growing season. Our PCA and sensitivity analyses revealed that
359 global radiation and soil temperature were the primary influencing factors of net CO_2-eq flux
360 variabilities. More specifically, we found that clouds (indicated by low R_g) strongly reduced the
361 net CO_2-eq uptake by blocking the incoming solar radiation and thus primarily reducing
362 photosynthesis [*Alton*, 2008]. Meanwhile, precipitation could also stimulate soil respiration
363 during the drier years (e.g., 2015 in this study) due to the increased soil moisture and thus
364 contributed to the overall reduced net CO_2 uptake [*Öquist et al.*, 2014; *Yuan et al.*, 2014].

Additionally, the higher SWC during the soil thawing and winter periods in 2015 could have stimulated CO_2 and CH_4 emissions from the peatland compared to the other two years (Figures S6&8).

Low soil temperature was expected to slow down the processes of photosynthesis, ecosystem respiration, and CH_4 production simultaneously in peatland ecosystems. However, the positive correlation between T_{soil} and net CO_2-eq uptake during the growing season indicated its primary role in enhancing photosynthesis relative to CO_2 and CH_4 emissions at the alpine peatlands in the QTP region [*Hao et al.*, 2011]. This also explained the between-year variability of net CO_2-eq uptake (Figures S6-9). Indeed, the observed positive effect of T_{soil} on CH_4 emissions, which has been widely found in this region [e.g., *Chen et al.*, 2008; *Song et al.*, 2015] and worldwide [e.g., *Dalmagro et al.*, 2019; *Drollinger et al.*, 2019; *Treat et al.*, 2014; *Zhao et al.*, 2016], amplified the sensitivity of net CO_2-eq emission to T_{soil} during the non-growing season but did not switch the overall relationship between net CO_2-eq and T_{soil} during the growing season.

Furthermore, the net CO_2-eq uptake was inhibited under hot and dry conditions (i.e., high VPD) as a result of the declined CH_4 emissions and net CO_2 uptake (Figure S3-4). As CO_2 and CH_4 fluxes were tightly coupled at daily and monthly scales due to their strong connection in biogeochemical processes, we also found that higher CO_2 uptake could lead to higher CH_4 production in peatland ecosystems, most likely due to the promoted root exudates [*Hatala et al.*, 2012; *Shoemaker et al.*, 2012]. Therefore, it is critical to investigate the environmental controls on the net CO_2-eq flux that integrated the soil biogeochemical and plant physiological processes and thus provided an overall view of how the changing environmental conditions in peatland ecosystems affected the net C and GHG balances.

388

389 4.3. C and GHG budgets of alpine peatlands on the QTP under global change

390 The alpine peatlands on the QTP typically act as net C sinks considering the C gains and losses
391 involved in the biogeochemical and physiological processes in the peatland ecosystem [*Chen et*
392 *al.*, 2014; *X Liu et al.*, 2019]. However, peatlands can be strong sources of net CO_2-eq and thus
393 result in net positive radiative forcing while taking the GWP and SGWP of other greenhouse
394 gases into account. As peatlands in this region could also be significant sources of N_2O [e.g.,
395 *Chen et al.*, 2013; *H Liu et al.*, 2019; *Marushchak et al.*, 2011], which has 265 times stronger
396 GWP than CO_2, the net positive radiative forcing of alpine peatlands on QTP would be further
397 enhanced if combining N_2O flux into the GHG budget. One recent model study also showed
398 similar results to this study that the significant CH_4 emissions from wetlands even offset the
399 entire regional GHG balance on the QTP [*Jin et al.*, 2015]. Therefore, the non-CO_2 GHG
400 emissions from peatlands play an important role in the regional GHG budgets by potentially
401 switching the alpine peatlands from a radiative cooling to a warming effect.

402 The C and GHG balances of the Ruoergai peatland are sensitive to the rapid climate
403 warming on the QTP, which has been widely observed during the last decades [*Yang et al.*, 2014;
404 *Yao et al.*, 2012; *You et al.*, 2016]. As the warmer temperature has been found to accelerate CH_4
405 emissions from peatlands in the Ruoergai Basin by promoting both anaerobic and aerobic
406 metabolisms [*Cui et al.*, 2015; *Yang et al.*, 2014], it is expected that the Ruoergai peatland will
407 emit more CH_4 to the atmosphere and result in more offsetting to both the radiative cooling
408 effect and the carbon sink strength of peatland ecosystems in the warmer scenarios. In addition,
409 glacier melting and permafrost thawing in response to the rising temperature could lead to more

410 peatland formations in this region [*Luan et al.*, 2018; *Yao et al.*, 2012], which will create more
411 CH_4 emission hotspots in the future.

412 The Ruoergai peatland is also challenged by drainage resulting from both increasing
413 human disturbances and intensified headward erosion of large numbers of tributaries. Many
414 peatlands have been drained for animal husbandry or mined for fuels primarily due to the
415 growing population (1.5 times larger) in the Ruoergai Basin since the 1960s [*Yao et al.*, 2011],
416 resulting in 18-31% of peatland degradation [*Chen et al.*, 2014; *Yao et al.*, 2011]. Besides, rapid
417 increases in runoff have caused many river diversions and thus incised an extensive amount of
418 peatlands, leading to enhanced peatland degradation [*Li et al.*, 2015]. Drainage can further alter
419 the GHG and C balances by affecting hydrology, soil, and vegetation composition in the
420 degraded peatland ecosystems [*Gyimah et al.*, 2020]. For example, the increased soil temperature
421 and decreased soil water content associated with peatland drainage could reduce CH_4 emissions
422 and net CO_2 uptake in the QTP region [*Yang et al.*, 2014; *Yang et al.*, 2017; *Zhou et al.*, 2017],
423 which would strengthen the positive radiative forcing of the alpine peatlands in this region.
424 Therefore, investigations on the effects of peatland drainage and restoration are greatly needed to
425 identify the role of alpine peatlands in regional and global C and GHG cycles under the
426 circumstances of climate change and anthropogenic disturbances in the future.
427

428 **5. Conclusions**

429 During the study period, our 2.5-year continuous eddy covariance flux measurements showed
430 that the typical alpine peatland on the eastern QTP acted as a net sink for atmospheric CO_2, a net
431 CH_4 source, and an overall net C sink. When considering their potential influence on radiative
432 forcing, the CH_4 emissions considerably offset the radiative cooling effect of the peatland net

CO_2 uptake, thus altering the peatland to a net CO_2-eq source and causing a potentially warming effect. Our analysis further demonstrated that global radiation and soil temperature were the main environmental drivers that influenced the alpine peatland net CO_2-eq flux variabilities from half-hourly to annual time scales. Besides, we found that both CH_4 and CO_2 emissions during the soil freezing and winter periods have contributed significantly to the annual net CO_2-eq fluxes, suggesting that the non-growing season C emissions are extremely important for assessing the overall C and GHG budgets of the alpine peatlands in the QTP region, particularly in a warming climate. The extended long-term continuous GHG monitoring is advocated to further investigate the feedback between the alpine peatlands and global change.

Acknowledgments

This research was funded by the Strategic Priority Research Program of Chinese Academy of Sciences (Grant No. XDB40010300), the National Natural Science Foundation of China (Grant Nos. 41907288, 41673119, and 41773140), and the Science and Technology Foundation of Guizhou Province (Grant Nos. [2019]1317 and [2020]1Y193). H. P. was supported by the "Light of West China" Program and the CAS Scholarship. J. C. gratefully acknowledges funding from the Kempe Foundations (grant no. SMK-1743).

Data availability statement

Datasets and codes for this research will be available at the GitHub repository link https://github.com/HaijunPeng/Carbon-balance-QTP-peatland upon publication.

References

456 Alm, J., S. Saarnio, H. Nykänen, J. Silvola, and P. J. Martikainen (1999), Winter CO_2, CH_4 and
457 N_2O fluxes on some natural and drained boreal peatlands, Biogeochemistry, 44(2), 163-
458 186, doi: 10.1023/A:1006074606204.
459 Alton, P. B. (2008), Reduced carbon sequestration in terrestrial ecosystems under overcast skies
460 compared to clear skies, Agric. For. Meteorol., 148(10), 1641-1653, doi:
461 10.1016/j.agrformet.2008.05.014.
462 Aurela, M., T. Laurila, and J.-P. Tuovinen (2002), Annual CO_2 balance of a subarctic fen in
463 northern Europe: Importance of the wintertime efflux, J. Geophys. Res. Atmos.,
464 107(D21), doi: 10.1029/2002jd002055.
465 Baldocchi, D., and J. Penuelas (2019), The physics and ecology of mining carbon dioxide from
466 the atmosphere by ecosystems, Global Change Biol., 25(4), 1191-1197, doi:
467 10.1111/gcb.14559.
468 Bridgham, S. D., H. Cadillo-Quiroz, J. K. Keller, and Q. Zhuang (2013), Methane emissions
469 from wetlands: biogeochemical, microbial, and modeling perspectives from local to
470 global scales, Global Change Biol., 19(5), 1325-1346, doi: 10.1111/gcb.12131.
471 Carlson, K. M., L. M. Curran, G. P. Asner, A. M. Pittman, S. N. Trigg, and J. Marion Adeney
472 (2013), Carbon emissions from forest conversion by Kalimantan oil palm plantations,
473 Nat. Clim. Change, 3(3), 283-287, doi: 10.1038/nclimate1702.
474 Chaudhary, N., P. A. Miller, and B. Smith (2017), Modelling past, present and future peatland
475 carbon accumulation across the pan-Arctic region, Biogeosciences, 14(18), 4023-4044,
476 doi: 10.5194/bg-14-4023-2017.
477 Chen, H., S. Yao, N. Wu, Y. Wang, P. Luo, J. Tian, Y. Gao, and G. Sun (2008), Determinants
478 influencing seasonal variations of methane emissions from alpine wetlands in Zoige

Plateau and their implications, J. Geophys. Res. Atmos., 113(D12), doi: 10.1029/2006jd008072.

Chen, H., X. Liu, D. Xue, D. Zhu, W. Zhan, W. Li, N. Wu, and G. Yang (2021), Methane emissions during different freezing-thawing periods from a fen on the Qinghai-Tibetan Plateau: Four years of measurements, Agric. For. Meteorol., 297, 108279, doi: 10.1016/j.agrformet.2020.108279.

Chen, H., et al. (2014), The carbon stock of alpine peatlands on the Qinghai-Tibetan Plateau during the Holocene and their future fate, Quat. Sci. Rev., 95, 151-158, doi: 10.1016/j.quascirev.2014.05.003.

Chen, H., et al. (2013), The impacts of climate change and human activities on biogeochemical cycles on the Qinghai-Tibetan Plateau, Global Change Biol., 19(10), 2940-2955, doi: 10.1111/gcb.12277.

Commane, R., et al. (2017), Carbon dioxide sources from Alaska driven by increasing early winter respiration from Arctic tundra, PNAS, 114(21), 5361-5366, doi: 10.1073/pnas.1618567114.

Cui, M., A. Ma, H. Qi, X. Zhuang, G. Zhuang, and G. Zhao (2015), Warmer temperature accelerates methane emissions from the Zoige wetland on the Tibetan Plateau without changing methanogenic community composition, Sci. Rep., 5(1), 11616, doi: 10.1038/srep11616.

Dalmagro, H. J., P. H. Zanella de Arruda, G. L. Vourlitis, M. J. Lathuillière, J. de S. Nogueira, E. G. Couto, and M. S. Johnson (2019), Radiative forcing of methane fluxes offsets net carbon dioxide uptake for a tropical flooded forest, Global Change Biol., 25(6), 1967-1981, doi: 10.1111/gcb.14615.

502 Dommain, R., S. Frolking, A. Jeltsch-Thömmes, F. Joos, J. Couwenberg, and P. H. Glaser
503 (2018), A radiative forcing analysis of tropical peatlands before and after their conversion
504 to agricultural plantations, Global Change Biol., 24(11), 5518-5533, doi:
505 10.1111/gcb.14400.
506 Drollinger, S., A. Maier, and S. Glatzel (2019), Interannual and seasonal variability in carbon
507 dioxide and methane fluxes of a pine peat bog in the Eastern Alps, Austria, Agric. For.
508 Meteorol., 275, 69-78, doi: 10.1016/j.agrformet.2019.05.015.
509 Fan, S. M., S. C. Wofsy, P. S. Bakwin, D. J. Jacob, and D. R. Fitzjarrald (1990), Atmosphere-
510 biosphere exchange of CO_2 and O_3 in the central Amazon forest, J. Geophys. Res.
511 Atmos., 95(D10), 16851-16864, doi: 10.1029/JD095iD10p16851.
512 Fenner, N., and C. Freeman (2011), Drought-induced carbon loss in peatlands, Nat. Geosci.,
513 4(12), 895-900, doi: 10.1038/ngeo1323.
514 Friedlingstein, P., et al. (2019), Global carbon budget 2019, Earth Syst. Sci. Data, 11(4), 1783-
515 1838, doi: 10.5194/essd-11-1783-2019.
516 Frolking, S., J. Talbot, M. C. Jones, C. C. Treat, J. B. Kauffman, E.-S. Tuittila, and N. Roulet
517 (2011), Peatlands in the Earth's 21st century climate system, Environ. Rev., 19, 371-396,
518 doi: 10.1139/a11-014.
519 Gash, J. H. C., and A. D. Culf (1996), Applying a linear detrend to eddy correlation data in
520 realtime, Boundary Layer Meteorol., 79(3), 301-306, doi: 10.1007/bf00119443.
521 Gorham, E. (1991), Northern peatlands: Role in the carbon cycle and probable responses to
522 climatic warming, Ecol. Appl., 1(2), 182-195, doi: 10.2307/1941811.

523 Gyimah, A., J. Wu, R. Scott, and Y. Gong (2020), Agricultural drainage increases the
524 photosynthetic capacity of boreal peatlands, Agric. Ecosyst. Environ., 300, 106984, doi:
525 10.1016/j.agee.2020.106984.
526 Hao, Y. B., X. Y. Cui, Y. F. Wang, X. R. Mei, X. M. Kang, N. Wu, P. Luo, and D. Zhu (2011),
527 Predominance of precipitation and temperature controls on ecosystem CO_2 exchange in
528 Zoige Alpine Wetlands of southwest China, Wetlands, 31(2), 413-422, doi:
529 10.1007/s13157-011-0151-1.
530 Hatala, J. A., M. Detto, and D. D. Baldocchi (2012), Gross ecosystem photosynthesis causes a
531 diurnal pattern in methane emission from rice, Geophys. Res. Lett., 39(6), doi:
532 10.1029/2012gl051303.
533 Hemes, K. S., S. D. Chamberlain, E. Eichelmann, S. H. Knox, and D. D. Baldocchi (2018), A
534 biogeochemical compromise: The high methane cost of sequestering carbon in restored
535 wetlands, Geophys. Res. Lett., 45(12), 6081-6091, doi: 10.1029/2018GL077747.
536 Hemes, K. S., S. D. Chamberlain, E. Eichelmann, T. Anthony, A. Valach, K. Kasak, D. Szutu, J.
537 Verfaillie, W. L. Silver, and D. D. Baldocchi (2019), Assessing the carbon and climate
538 benefit of restoring degraded agricultural peat soils to managed wetlands, Agric. For.
539 Meteorol., 268, 202-214, doi: 10.1016/j.agrformet.2019.01.017.
540 Hong, Y. T., B. Hong, Q. H. Lin, Y. Shibata, M. Hirota, Y. X. Zhu, X. T. Leng, Y. Wang, H.
541 Wang, and L. Yi (2005), Inverse phase oscillations between the East Asian and Indian
542 Ocean summer monsoons during the last 12000 years and paleo-El Niño, Earth Planet.
543 Sci. Lett., 231(3), 337-346, doi: 10.1016/j.epsl.2004.12.025.

544 Hopple, A. M., R. M. Wilson, M. Kolton, C. A. Zalman, J. P. Chanton, J. Kostka, P. J. Hanson,
545 J. K. Keller, and S. D. Bridgham (2020), Massive peatland carbon banks vulnerable to
546 rising temperatures, Nat. Commun., 11(1), 2373, doi: 10.1038/s41467-020-16311-8.
547 Jin, Z., Q. Zhuang, J.-S. He, X. Zhu, and W. Song (2015), Net exchanges of methane and carbon
548 dioxide on the Qinghai-Tibetan Plateau from 1979 to 2100, Environ. Res. Lett., 10(8),
549 085007, doi: 10.1088/1748-9326/10/8/085007.
550 Kirschke, S., et al. (2013), Three decades of global methane sources and sinks, Nat. Geosci.,
551 6(10), 813-823, doi: 10.1038/ngeo1955.
552 Kljun, N., P. Calanca, M. W. Rotach, and H. P. Schmid (2015), A simple two-dimensional
553 parameterisation for Flux Footprint Prediction (FFP), Geosci. Model Dev., 8(11), 3695-
554 3713, doi: 10.5194/gmd-8-3695-2015.
555 Li, Z.-W., Z.-Y. Wang, G. Brierley, T. Nicoll, B.-Z. Pan, and Y.-F. Li (2015), Shrinkage of the
556 Ruoergai Swamp and changes to landscape connectivity, Qinghai-Tibet Plateau, Catena,
557 126, 155-163, doi: 10.1016/j.catena.2014.10.035.
558 Liu, H., D. Zak, F. Rezanezhad, and B. Lennartz (2019), Soil degradation determines release of
559 nitrous oxide and dissolved organic carbon from peatlands, Environ. Res. Lett., 14(9),
560 094009, doi: 10.1088/1748-9326/ab3947.
561 Liu, J., Y. Zhou, A. Valach, R. Shortt, K. Kasak, C. Rey-Sanchez, K. S. Hemes, D. Baldocchi,
562 and D. Y. F. Lai (2020), Methane emissions reduce the radiative cooling effect of a
563 subtropical estuarine mangrove wetland by half, Global Change Biol., doi:
564 10.1111/gcb.15247.
565 Liu, X., D. Zhu, W. Zhan, H. Chen, Q. Zhu, Y. Hao, W. Liu, and Y. He (2019), Five-year
566 measurements of net ecosystem CO_2 exchange at a fen in the Zoige peatlands on the

Qinghai-Tibetan Plateau, J. Geophys. Res. Atmos., 124(22), 11803-11818, doi: 10.1029/2019jd031429.

Loisel, J., S. van Bellen, L. Pelletier, J. Talbot, G. Hugelius, D. Karran, Z. Yu, J. Nichols, and J. Holmquist (2017), Insights and issues with estimating northern peatland carbon stocks and fluxes since the Last Glacial Maximum, Earth-Sci. Rev., 165, 59-80, doi: 10.1016/j.earscirev.2016.12.001.

Luan, J., S. Liu, J. Wu, M. Wang, and Z. Yu (2018), The transient shift of driving environmental factors of carbon dioxide and methane fluxes in Tibetan peatlands before and after hydrological restoration, Agric. For. Meteorol., 250-251, 138-146, doi: 10.1016/j.agrformet.2017.12.248.

Lund, M., et al. (2010), Variability in exchange of CO_2 across 12 northern peatland and tundra sites, Global Change Biol., 16(9), 2436-2448, doi: 10.1111/j.1365-2486.2009.02104.x.

Marushchak, M. E., A. Pitkämäki, H. Koponen, C. Biasi, M. Seppälä, and P. J. Martikainen (2011), Hot spots for nitrous oxide emissions found in different types of permafrost peatlands, Global Change Biol., 17(8), 2601-2614, doi: 10.1111/j.1365-2486.2011.02442.x.

Mastepanov, M., C. Sigsgaard, E. J. Dlugokencky, S. Houweling, L. Ström, M. P. Tamstorf, and T. R. Christensen (2008), Large tundra methane burst during onset of freezing, Nature, 456(7222), 628-630, doi: 10.1038/nature07464.

Mauder, M., and T. Foken (2004), Documentation and instruction manual of the eddy covariance software package TK2, 1-67.

588 Moncrieff, J., R. Clement, J. Finnigan, and T. Meyers (2004), Averaging, Detrending, and
589 Filtering of Eddy Covariance Time Series, in Handbook of Micrometeorology, edited by
590 X. Lee, W. J. Massman and B. E. Law, Springer Netherlands.
591 Moncrieff, J. B., J. M. Massheder, H. de Bruin, J. Elbers, T. Friborg, B. Heusinkveld, P. Kabat,
592 S. Scott, H. Soegaard, and A. Verhoef (1997), A system to measure surface fluxes of
593 momentum, sensible heat, water vapour and carbon dioxide, J. Hydrol., 188-189(0), 589-
594 611, doi: 10.1016/S0022-1694(96)03194-0.
595 Myhre, G., et al. (2013), Anthropogenic and Natural Radiative Forcing, in Climate Change 2013:
596 The Physical Science Basis. Contribution of Working Group I to the Fifth Assessment
597 Report of the Intergovernmental Panel on Climate Change, edited by T. F. Stocker, D.
598 Qin, G.-K. Plattner, M. Tignor, S. K. Allen, J. Boschung, A. Nauels, Y. Xia, V. Bex and
599 P. M. Midgley, Cambridge University Press, Cambridge, United Kingdom and New
600 York, NY, USA.
601 Natali, S. M., et al. (2019), Large loss of CO_2 in winter observed across the northern permafrost
602 region, Nat. Clim. Change, doi: 10.1038/s41558-019-0592-8.
603 Neubauer, S. C., and J. P. Megonigal (2015), Moving Beyond Global Warming Potentials to
604 Quantify the Climatic Role of Ecosystems, Ecosystems, 18(6), 1000-1013, doi:
605 10.1007/s10021-015-9879-4.
606 Nilsson, M., J. Sagerfors, I. Buffam, H. Laudon, T. Eriksson, A. Grelle, L. Klemedtsson, P. E. R.
607 Weslien, and A. Lindroth (2008), Contemporary carbon accumulation in a boreal
608 oligotrophic minerogenic mire – a significant sink after accounting for all C-fluxes,
609 Global Change Biol., 14(10), 2317-2332, doi: 10.1111/j.1365-2486.2008.01654.x.

Nugent, K. A., I. B. Strachan, N. T. Roulet, M. Strack, S. Frolking, and M. Helbig (2019), Prompt active restoration of peatlands substantially reduces climate impact, Environ. Res. Lett., 14(12), 124030, doi: 10.1088/1748-9326/ab56e6.

Öquist, M. G., K. Bishop, A. Grelle, L. Klemedtsson, S. J. Köhler, H. Laudon, A. Lindroth, M. Ottosson Löfvenius, M. B. Wallin, and M. B. Nilsson (2014), The full annual carbon balance of boreal forests is highly sensitive to precipitation, Environ. Sci. Technol. Lett., 1(7), 315-319, doi: 10.1021/ez500169j.

Papale, D., et al. (2006), Towards a standardized processing of Net Ecosystem Exchange measured with eddy covariance technique: algorithms and uncertainty estimation, Biogeosciences, 3(4), 571-583, doi: 10.5194/bg-3-571-2006.

Peichl, M., M. Öquist, M. O. Löfvenius, U. Ilstedt, J. Sagerfors, A. Grelle, A. Lindroth, and M. B. Nilsson (2014), A 12-year record reveals pre-growing season temperature and water table level threshold effects on the net carbon dioxide exchange in a boreal fen, Environ. Res. Lett., 9(5), 055006, doi: 10.1088/1748-9326/9/5/055006.

Peng, H., B. Hong, Y. Hong, Y. Zhu, C. Cai, L. Yuan, and Y. Wang (2015), Annual ecosystem respiration variability of alpine peatland on the eastern Qinghai–Tibet Plateau and its controlling factors, Environ. Monit. Assess., 187(9), 550, doi: 10.1007/s10661-015-4733-x.

Peng, H., Q. Guo, H. Ding, B. Hong, Y. Zhu, Y. Hong, C. Cai, Y. Wang, and L. Yuan (2019), Multi-scale temporal variation in methane emission from an alpine peatland on the Eastern Qinghai-Tibetan Plateau and associated environmental controls, Agric. For. Meteorol., 276-277, 107616, doi: 10.1016/j.agrformet.2019.107616.

632 Petrescu, A. M. R., et al. (2015), The uncertain climate footprint of wetlands under human
633 pressure, PNAS, 112(15), 4594-4599, doi: 10.1073/pnas.1416267112.
634 Poulter, B., et al. (2017), Global wetland contribution to 2000-2012 atmospheric methane growth
635 rate dynamics, Environ. Res. Lett., 12(9), 094013, doi: 10.1088/1748-9326/aa8391.
636 Reichstein, M., et al. (2005), On the separation of net ecosystem exchange into assimilation and
637 ecosystem respiration: Review and improved algorithm, Global Change Biol., 11(9),
638 1424-1439, doi: 10.1111/j.1365-2486.2005.001002.x.
639 Rinne, J., et al. (2018), Temporal variation of ecosystem scale methane emission from a boreal
640 fen in relation to temperature, water table position, and carbon dioxide fluxes, Global
641 Biogeochem. Cycles, 32(7), 1087-1106, doi: 10.1029/2017GB005747.
642 Schaefer, H., et al. (2016), A 21st-century shift from fossil-fuel to biogenic methane emissions
643 indicated by $^{13}CH_4$, Science, 352(6281), 80-84, doi: 10.1126/science.aad2705.
644 Shoemaker, J. K., R. K. Varner, and D. P. Schrag (2012), Characterization of subsurface
645 methane production and release over 3 years at a New Hampshire wetland, Geochim.
646 Cosmochim. Acta, 91, 120-139, doi: 10.1016/j.gca.2012.05.029.
647 Slättberg, N., and D. Chen (2020), A long-term climatology of planetary boundary layer height
648 over the Tibetan Plateau revealed by ERA5, paper presented at EGU General Assembly
649 2020, Online.
650 Song, C., et al. (2020), A microbial functional group-based CH_4 model integrated into a
651 terrestrial ecosystem model: model structure, site-level evaluation, and sensitivity
652 analysis, J. Adv. Model. Earth Syst., 12(4), e2019MS001867, doi:
653 10.1029/2019ms001867.

654 Song, W., H. Wang, G. Wang, L. Chen, Z. Jin, Q. Zhuang, and J.-S. He (2015), Methane
655 emissions from an alpine wetland on the Tibetan Plateau: Neglected but vital contribution
656 of the nongrowing season, J. Geophys. Res. Biogeosci., 120(8), 1475-1490, doi:
657 10.1002/2015jg003043.
658 Stocker, B. D., Z. Yu, C. Massa, and F. Joos (2017), Holocene peatland and ice-core data
659 constraints on the timing and magnitude of CO_2 emissions from past land use, PNAS,
660 114(7), 1492-1497, doi: 10.1073/pnas.1613889114.
661 Swindles, G. T., et al. (2019), Widespread drying of European peatlands in recent centuries, Nat.
662 Geosci., 12(11), 922-928, doi: 10.1038/s41561-019-0462-z.
663 Tang, L., X. Duan, F. Kong, F. Zhang, Y. Zheng, Z. Li, Y. Mei, Y. Zhao, and S. Hu (2018),
664 Influences of climate change on area variation of Qinghai Lake on Qinghai-Tibetan
665 Plateau since 1980s, Sci. Rep., 8(1), 7331, doi: 10.1038/s41598-018-25683-3.
666 Treat, C. C., W. M. Wollheim, R. K. Varner, A. S. Grandy, J. Talbot, and S. Frolking (2014),
667 Temperature and peat type control CO_2 and CH_4 production in Alaskan permafrost peats,
668 Global Change Biol., 20(8), 2674-2686, doi: 10.1111/gcb.12572.
669 Turetsky, M. R., B. Benscoter, S. Page, G. Rein, G. R. van der Werf, and A. Watts (2015),
670 Global vulnerability of peatlands to fire and carbon loss, Nat. Geosci., 8(1), 11-14, doi:
671 10.1038/ngeo2325.
672 Turetsky, M. R., et al. (2014), A synthesis of methane emissions from 71 northern, temperate,
673 and subtropical wetlands, Global Change Biol., 20(7), 2183-2197, doi:
674 doi:10.1111/gcb.12580.

675 Turunen, J., E. Tomppo, K. Tolonen, and A. Reinikainen (2002), Estimating carbon
676 accumulation rates of undrained mires in Finland-application to boreal and subarctic
677 regions, The Holocene, 12(1), 69-80, doi: 10.1191/0959683602hl522rp.
678 Ueyama, M., T. Yazaki, T. Hirano, Y. Futakuchi, and M. Okamura (2020), Environmental
679 controls on methane fluxes in a cool temperate bog, Agric. For. Meteorol., 281, 107852,
680 doi: 10.1016/j.agrformet.2019.107852.
681 Wang, M., et al. (2015), Higher recent peat C accumulation than that during the Holocene on the
682 Zoige Plateau, Quat. Sci. Rev., 114, 116-125, doi: 10.1016/j.quascirev.2015.01.025.
683 Webb, E. K., G. I. Pearman, and R. Leuning (1980), Correction of flux measurements for density
684 effects due to heat and water-vapor transfer, Q. J. R. Meteorolog. Soc., 106(447), 85-100,
685 doi: 10.1002/qj.49710644707.
686 Wilczak, J. M., S. P. Oncley, and S. A. Stage (2001), Sonic anemometer tilt correction
687 algorithms, Boundary Layer Meteorol., 99(1), 127-150, doi: 10.1023/a:1018966204465.
688 WMO (2018), WMO Greenhouse Gas Bulletin No. 14: The State of Greenhouse Gases in the
689 Atmosphere Based on Global Observations through 2017.
690 Wutzler, T., A. Lucas-Moffat, M. Migliavacca, J. Knauer, K. Sickel, L. Šigut, O. Menzer, and
691 M. Reichstein (2018), Basic and extensible post-processing of eddy covariance flux data
692 with REddyProc, Biogeosciences, 15(16), 5015-5030, doi: 10.5194/bg-15-5015-2018.
693 Xiang, S., R. Guo, N. Wu, and S. Sun (2009), Current status and future prospects of Zoige Marsh
694 in Eastern Qinghai-Tibet Plateau, Ecol. Eng., 35(4), 553-562, doi:
695 10.1016/j.ecoleng.2008.02.016.

696 Xu, J., P. J. Morris, J. Liu, and J. Holden (2018), PEATMAP: Refining estimates of global
697 peatland distribution based on a meta-analysis, Catena, 160, 134-140, doi:
698 10.1016/j.catena.2017.09.010.
699 Yang, G., H. Chen, N. Wu, J. Tian, C. Peng, Q. Zhu, D. Zhu, Y. He, Q. Zheng, and C. Zhang
700 (2014), Effects of soil warming, rainfall reduction and water table level on CH_4 emissions
701 from the Zoige peatland in China, Soil Biol. Biochem., 78, 83-89, doi:
702 10.1016/j.soilbio.2014.07.013.
703 Yang, G., et al. (2017), Qinghai–Tibetan Plateau peatland sustainable utilization under
704 anthropogenic disturbances and climate change, Ecosyst. Health Sustainability, 3(3),
705 e01263, doi: 10.1002/ehs2.1263.
706 Yao, L., Y. Zhao, S. Gao, J. Sun, and F. Li (2011), The peatland area change in past 20 years in
707 the Zoige Basin, eastern Tibetan Plateau, Front. Earth Sci., 5(3), 271, doi:
708 10.1007/s11707-011-0178-x.
709 Yao, T., et al. (2012), Different glacier status with atmospheric circulations in Tibetan Plateau
710 and surroundings, Nat. Clim. Change, 2(9), 663-667, doi: 10.1038/nclimate1580.
711 You, Q., J. Min, and S. Kang (2016), Rapid warming in the Tibetan Plateau from observations
712 and CMIP5 models in recent decades, Int. J. Climatol., 36(6), 2660-2670, doi:
713 10.1002/joc.4520.
714 Yu, Z., J. Loisel, D. P. Brosseau, D. W. Beilman, and S. J. Hunt (2010), Global peatland
715 dynamics since the Last Glacial Maximum, Geophys. Res. Lett., 37(13), doi:
716 10.1029/2010gl043584.

717 Yuan, W., et al. (2014), Multiyear precipitation reduction strongly decreases carbon uptake over
718 northern China, J. Geophys. Res. Biogeosci., 119(5), 881-896, doi:
719 10.1002/2014jg002608.
720 Yuan, W., et al. (2011), Thermal adaptation of net ecosystem exchange, Biogeosciences, 8(6),
721 1453-1463, doi: 10.5194/bg-8-1453-2011.
722 Yvon-Durocher, G., A. P. Allen, D. Bastviken, R. Conrad, C. Gudasz, A. St-Pierre, N. Thanh-
723 Duc, and P. A. del Giorgio (2014), Methane fluxes show consistent temperature
724 dependence across microbial to ecosystem scales, Nature, 507(7493), 488-491, doi:
725 10.1038/nature13164.
726 Zhao, J., M. Peichl, and M. B. Nilsson (2016), Enhanced winter soil frost reduces methane
727 emission during the subsequent growing season in a boreal peatland, Global Change
728 Biol., 22(2), 750-762, doi: 10.1111/gcb.13119.
729 Zhao, Y., Y. Tang, Z. Yu, H. Li, B. Yang, W. Zhao, F. Li, and Q. Li (2014), Holocene peatland
730 initiation, lateral expansion, and carbon dynamics in the Zoige Basin of the eastern
731 Tibetan Plateau, The Holocene, 24(9), 1137-1145, doi: 10.1177/0959683614538077.
732 Zhou, W., L. Cui, Y. Wang, and W. Li (2017), Methane emissions from natural and drained
733 peatlands in the Zoigê, eastern Qinghai-Tibet Plateau, J. For. Res., 28(3), 539-547, doi:
734 10.1007/s11676-016-0343-x.